ISABE-2015-20102

Preliminary Design and Off-Design Optimization of a Single Stage Axial Compressor

Ibrahim Eryilmaz, Jean-François Brouckaert, Tom Verstraete, Zuheyr Alsalihi
Turbomachinery and Propulsion Department
von Karman Institute for Fluid Dynamics
Chaussee de Waterloo 72, Rhode Saint Genese 1640
Belgium

Abstract

This paper gives the introductory results of a new meridional optimization system for axial flow compressors related to research performed at the von Karman Institute. The study concentrates on the optimization of a single stage axial compressor by linking meridional design/analysis tools and evolutionary algorithms. The Nasa compressor Stage 35 was optimized in terms of primary design variables flowpath, loading distribution and solidity distribution to maximize two conflicting parameters namely stall margin and efficiency.

Two test cases, the high transonic Nasa Stage 35 and the EU FP6 Vital low pressure compressor stage were used for validating the throughflow. Comparison of different loss models show that successful designs and predictions can be obtained if the correct groups of these models are implemented together.

Two optimization tasks were performed for the Nasa Stage 35 compressor. At first, the analysis mode optimization was used to improve the performance of the existing single stage. A further design mode optimization has extended the work to a more general solution by designing a new stage. Selected pareto-optimal geometries were investigated by 3-D Navier Stokes analysis to confirm improvements.

Nomenclature

OP	Operating point
PR	Pressure ratio
S	Stall point operation
SM	Stall margin
V	Velocity
h_o	Enthalpy
m	Mass flow rate
r	Radius
r_c	Radius of curvature
t	Tangential component
ϕ	Streamline angle
RPM	Rotational speed in revolution per minute
CFD	Computational fluid dynamics

Introduction

Conceptual design of gas turbine engines requires compressor flowpath which is an essential part of the total work that will affect the whole engine study. In preliminary design studies of gas turbine components where the annulus geometry and blading are defined for a given mass flow rate and pressure rise; mathematical models and throughflow tools are commonly used and these algorithms provide fast approximations to real three dimensional flow. At this step, improvements of stage characteristics like pressure rise, efficiency and stall margin will be obtained with minimum computational cost and time. Once the baseline compressor geometry has been defined, further improvements can be achieved with 3-D CFD calculations where the cost is much larger. It is due to the reduced cost that these models are alternatives to be coupled with optimization algorithms. Chen et al. [1] presented a study related to design optimization of a multistage axial compressor by using analytical relations between efficiency and fundamental flow parameters like flow coefficient, work coefficient and degree of reaction. These kind of mathematical models based on analytical relations give an idea to designers about the optimum flow angles for the turbomachine. Design optimization by direct solvers can be done either by high fidelity tools like CFD or with low fidelity tools based on throughflow methods. The order of comparison for computational cost is between hours and seconds. A design optimization study related to Nasa Rotor 37 compressor was done by Benini [2] by an optimization algorithm coupled with a three dimensional Navier Stokes code CFX-TASCflow. By keeping the flowpath fixed, the rotor blade profiles were parameterized as camberline and thickness distribution with Bezier polynomials. The rotor stage was optimized to maximize design point efficiency and pressure ratio. A design optimization study related to an existing 9 stage Rolls Royce compressor was presented by Keskin and Bestle [3] based on coupling a commercial optimizer iSight and a throughflow solver. The flowpath mean radius distribution, flowpath blade height distribution and streamwise stage pressure ratio distribution were the design variables to maximize overall compressor efficiency. Teichel et al. [4] presented a design optimization study

related to a single stage axial compressor by using two different throughflow tools. Obtaining higher stage pressure ratio was the optimization target and the improved values from throughflow results were in reasonable agreement with CFD.

Once an optimizer-solver coupled system is developed, it is possible to investigate every combination of design parameters and design objectives. The motivation behind the global objective of this study is to introduce optimization which is integrated to a fast throughflow solver for complete gas turbine multistage compression system design and off-design operation. For this study the target is restricted to developing the integrated solver-optimizer system mainly focusing on design and off-design performance of a single stage axial compressor.

Throughflow Code

The throughflow code used in the study is based on S1 and S2 calculation system that is proposed by Wu [5]. Losses in the S1 blade to blade plane are represented by loss correlations based on experimental results. The axisymmetric flow hub to tip solution is governed by the momentum equation in S2 radial - tangential plane which is named as the radial equilibrium equation.

Streamline movement in the meridional plane depends only on the radial density gradient, flowpath shape and non free vortex flow. Streamline movement due to blade thickness distribution and blade forces are not taken into account. Full radial equilibrium condition is given by Equation 1.

$$\frac{dh_o}{dr} = T\frac{ds}{dr} + V_t.\frac{dV_t}{dr} + \frac{V_t^2}{r} + V_m.\frac{dV_m}{dr} + \frac{V_m^2}{r_c}\cos\phi - V_m\frac{dV_m}{dm}\sin\phi \quad \textbf{Eqn:1}$$

After each iteration, streamlines are adjusted to guarantee the same mass flow rate at each stream tube. For streamline reposition, a relaxation factor is implemented. This relaxation factor defines the weighted average between the previous radius and new radius for the movable streamlines.

Losses due to viscous effects in the S1 blade to blade plane are represented by loss and deviation correlations. These loss and deviation correlations mostly depend on low speed cascade tests and deviate from real loss values at high speed operation. According to low speed cascade tests, losses are correlated to the diffusion factor which is a function of wake momentum thickness. Formulation for the diffusion factor is given by Lieblein et al. [6]. Attempts to validate loss predictions with respect to real operation have resulted in corrections to the loss correlations of cascade measurements. When losses are represented by two main sources, predictions come out with consistent values to real operation [7]. These two main contributors are diffusion factor losses and losses due to shock waves. Diffusion factor losses should be corrected with compressibility effects, incidence effects and also supersonic pockets appearing on blade due to operation between critical Mach number and sonic Mach number. For operation higher than sonic Mach number, the shock losses should be calculated.

Several profile loss models have been implemented. Profile loss model 1 and deviation model depends on the formulations of Aungier [8] which are also available in graphical form [17]. Profile loss model 2 is in graphical form and given by Creveling and Carmody [10]. This loss model gives an evolution of loss parameter as a function of radius which makes the loss model to include losses due to effect of hub and tip regions. Endwall loss is given by Howell [11] and tip clearence loss is given by Breugelmans and Colpin [16]. A comparison for application of these losses on Nasa Stage 35 rotor are given in Figure 1.

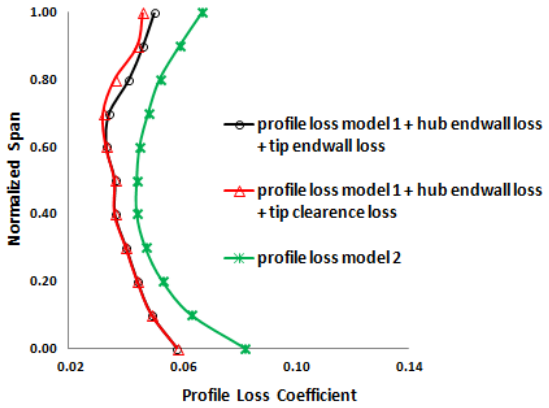

Figure 1 Profile Loss Models

For profile loss model 1 additional losses are introduced with a user input penetration depth. This dept represents how far the loss affects the flow field from hub or tip. This application adds an additional assumption for the loss model. Incidence and Mach number corrections for profile losses are implemented according to Aungier [8]. Blockage factor calculation is implemented according to method given by Pachidis [12].

Similar to the profile loss models, also several shock loss models have been implemented. Shock loss Model 1 is given in Pachidis [12] and Model 2 is given in Schwenk et al. [13]. For shock loss calculations, both models use the same principle given as bow shock wave in front of the passage and its extension as a passage shock in the adjacent blade is represented by an average Mach number; and the corresponding loss is evaluated with the assumption of normal shock attached to the leading edge. For shock loss model 1, the Prandtl Meyer expansion is calculated with the assumption of circular suction side geometry. For shock loss model 2, the Prandtl Meyer expansion angle which is equivalent to the supersonic turning is given as an input that

is a fraction of camber angle. A comparison for application of these losses on Nasa Stage 35 rotor are given in Figure 2. For a supersonic turning ratio equal to zero, shock Mach number is equal to inlet relative Mach number.

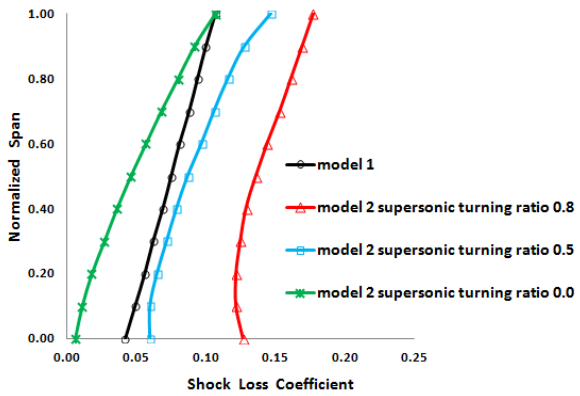

Figure 2 Shock Loss Models

Comparison of loss models in Figure 1 and Figure 2 show that, losses will differ from each other in terms of both magnitude and spanwise evolution. A throughflow program should allow the user to tune these models. Scaling factors are available in the throughflow code to tune loss models at every stagewise and spanwise calculation station. Due to different aerodynamic properties, each compressor requires different scaling factors and this tuning property brings an additional assumption in performance predictions. However the tuning option gives the possibility of making detailed changes in the preliminary design of a compressor where the flowpath and blading are almost defined.

The throughflow tool can opearate at two modes. Fırst type is the analysis mode operation. At analysis mode, the code requires flowpath and blading definitions. Blading is defined with parameters metal angles, chord lengths and blade numbers. For loss calculations, additional to the loss models the neccessary blading information is required like profile types, leading edge information, profile thickness and maximum camber location . For a given mass flow rate the code calculates the compressor performance. The validation studies of the throughflow with the two test case were done in the analysis mode operation. The second type is the design mode operation. For a given mass flow rate and pressure ratio, the code requires several inputs and designs a compressor stage or stages for a multistage task. Mass flow rate, inlet axial velocity, first stage hub to tip ratio are used to locate the flowpath at stage inlet; meridional view aspect ratios are used to locate calculation stations at blade inlet and outlet; pressure ratio, rotational speed and pressure ratio distribution are used to determine the neccessary angles for the required work input; solidity distributions are used for loss calculations and to determine the blade numbers; axial velocity ratio, meanline radius ratio and ratio of rotor area contraction to stage area contaraction are used to describe the flowpath. Similar to the analysis mode operation, blading information for loss models are also neccessary for the design mode operation. One design task is an internal iterative process and at every internal design task, analysis mode operation is called to the loop to check whether the target pressure ratio is obtained or not. According to the amount of error, the design mode is re-executed. The code can also design a compressor for a given flowpath and this option does not require the parameters which are used to describe the flowpath.

Throughflow Validation

There are two test cases available for the validation of throughflow. The first compressor stage is the Nasa Stage 35 [14] which is a rotor-stator configuration. The inlet relative Mach Number changes from 1.1 to 1.5 from hub to tip. Stage design pressure ratio and mass flow rate are reported as 1.82 and 20.1 kg/s. The second stage is VKI Vital low pressure compressor stage [15] which is an IGV-rotor-stator configuration for which the inlet relative Mach number is subsonic from hub to tip. The stage is in supercritical operation where supersonic pockets are possible on the rotor suction side.

To be used as a reference for the rest of the study a CFD validation was done by comparing 3-D Navier Stokes computation and experimental results [14] of Nasa Stage 35. Numeca Fine Turbo was used as the solver. The turbulence model is Spalart Allmaras and wall cell width is defined according to wall y+ to be around 1. Grid density is 0.6 million grid per blade row with 57 spanwise points. Grid dependence study showed that there is no significant difference when the grid size is increased to 1.5 million grid per blade row with 73 spanwise points. Effects of any other parameter such as turbulence model or numerical scheme was not investigated since the main focus of the study is on optimization with throughflow rather than CFD analysis. Figure 3 shows the spanwise total pressure loss coefficient distribution of Stage 35 rotor.

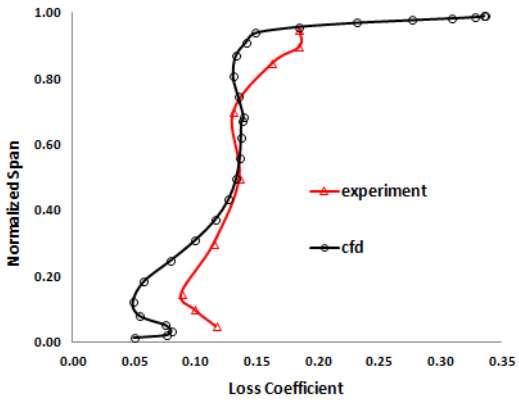

Figure 3 Stage 35 Rotor Loss Coefficient

With this distribution being close to experimental measurements, CFD is considered to be a validation tool for the throughflow code and final evaluation tool for optimized geometries. To be comparable with the throughflow calculations, the original bladings of these stages were changed to double circular arc blades (DCA). Calculations show that there is a stall margin and efficiency decrease in Stage 35 due to implementation of DCA blading in high transonic flow. Figure 4 shows the comparison between CFD and throughflow for outlet absolute total pressure distribution at Stage 35 rotor. The throughflow code is able to capture the trend with a deviation in magnitude.

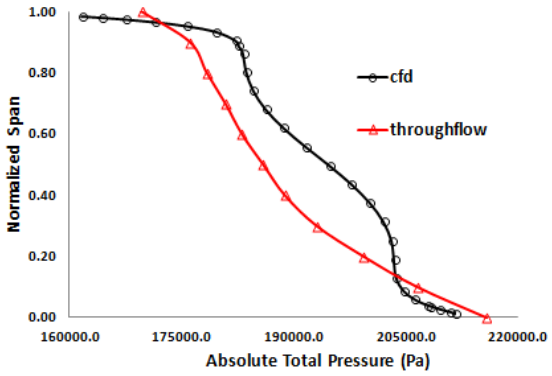

Figure 4 Rotor 35 Total Pressure Distribution

Isentropic Mach number distribution from CFD is calculated at 95 % spanwise location. Figure 5 shows the average Mach number coming from CFD calculation and throughflow calculation. This Mach number is the average between inlet relative Mach number and shock Mach number which is used in the shock loss calculation of Stage 35 rotor. Since the blading in the CFD was changed to a DCA blading, Mach number calculation of the throughflow with circular suction side assumption is consistent with CFD.

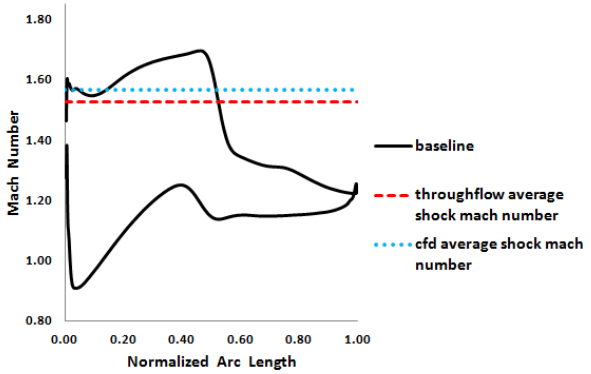

Figure 5 Stage 35 Blade Isentropic Mach Distribution

Second validation case is the Vital compressor. This low pressure compressor stage was designed for a counter-rotating turbofan engine architecture and stage performance measurements were reported by Brouckaert et al. [9]. The stage fall out of classical design range in terms of flow and loading coefficients due to lower rotational speed [9]. Experimental spanwise distributions of rotor total pressure and rotor total temperature were used to calculate rotor isentropic efficiency. It is found that the rotor has high losses at the endwall regions with a high value of loss penetration to the mid flow region. This unconventional design can be considered as a special test case to compare the un-tuned and tuned predictions of the throughflow code. The loss and deviation scaling factor distribution for the Vital rotor are given in Figure 6. The values are determined as a ratio of un-tuned predictions and CFD calculation.

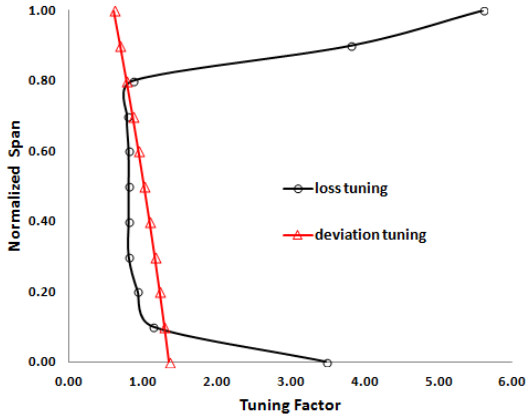

Figure 6 Vital Rotor Scaling Factor Distribution

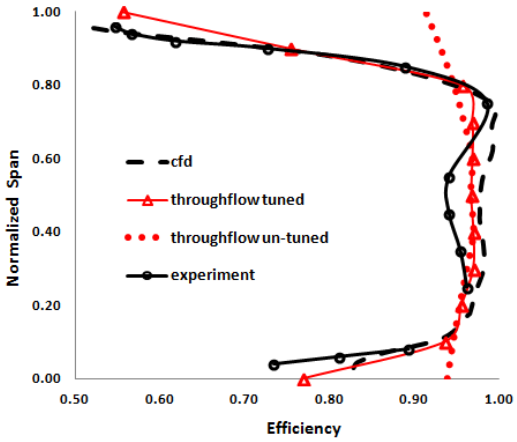

Figure 7 Vital Efficiency Distribution

Figure 7 gives the total to total isentropic efficiency distribution of the Vital low pressure compressor. Figure 8 gives the outlet meridional velocity distribution of Vital rotor. Figures 7 and 8 show the possibility of improvement in performance predictions when the throughflow is user tuned. Although each compressor needs different tuning

factors, this tuning option provides improved predictions for a certain type of compressor especially at design level when the flowpath and blading are almost defined.

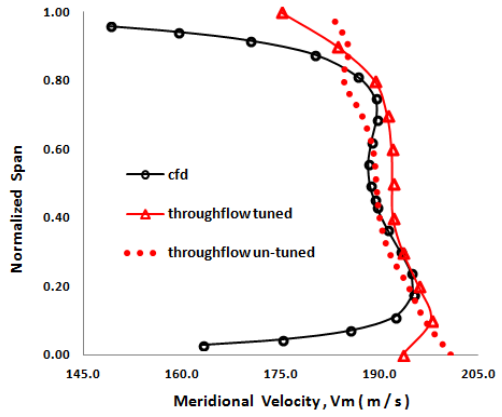

Figure 8 Vital Compressor Meridional Velocity

Multi-objective Formulation

A real valued genetic algorithm is used as optimization algorithm. A truncation selection is implemented after the fitness evaluation of each individual. The best performing population members are kept for the next generation. A Multi-objective formulation is obtained by maximizing the weighted sum of fitness values of individual design objectives. Rather than finding the stall point exactly with a stall criteria, the decision of increased stall margin depends on the capability of stage in doing higher pressure rise at a slightly reduced mass flow rate.

Analysis Mode Optimization

There are in total 11 design variables in the analysis mode optimization of Nasa Stage 35. Optimization variables are given in Table 1. Camber and chord distributions are represented by Bezier polynomials and the control points of Bezier polynomials are defined as optimization variables. Flowpath coordinates are fixed at the inlet and exit and flowpath contraction is controlled by a control point of a Bezier curve.

Table 1 Analysis Mode Optimization Variables

Optimization variables (11 variables)	# of variable
rotor camber distribution	4 control points
rotor chord distribution	4 control points
rotor blade number	1 value
flowpath control point @ tip	1 value
flowpath control point @ hub	1 value

In Figure 9 the pareto front obtained from the analysis mode optimization is given and pareto-optimum results are numbered from 1 to 5. Geometries 1,2 and 3 are stall margin dominant and geometries 4 and 5 are efficiency dominant. Effects of flowpath contraction on the optimization are presented in the Figure 10 and 11.

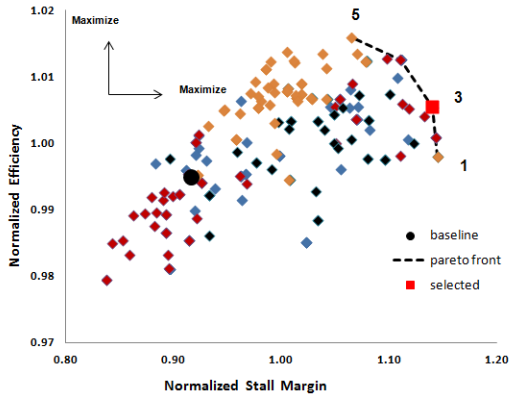

Figure 9 Analysis Mode Optimization Pareto Front

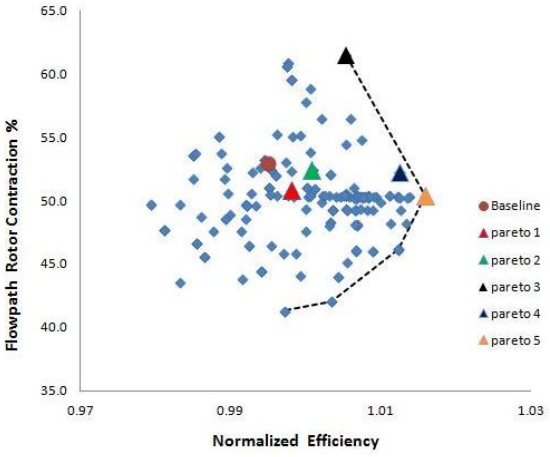

Figure 10 Flowpath Contraction vs Efficiency

According to Figure 10, there is an optimum flowpath rotor contraction that points to maximum efficiency and the efficiency dominated pareto optimum geometries are in the border of design space. According Figure 11, there are possible values of rotor flowpath contraction to maximize stall margin. Stall margin dominated pareto-optimum geometries are in the border of the design space. The same comments are valid for the tip solidity. This implies that stall margin is a combined effect of the design variables.

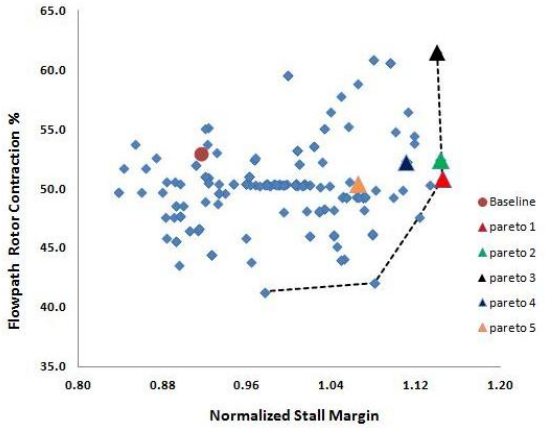

Figure 11: Flowpath Contraction vs. Stall Margin

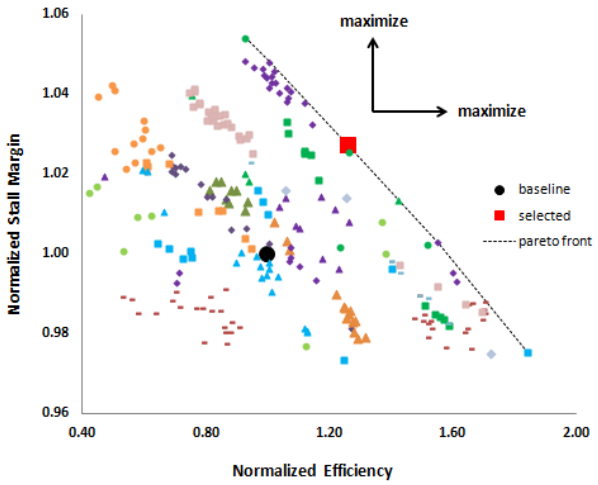

Figure 12 Design Mode Optimization Pareto Front

Design Mode Optimization

There are in total 23 design variables in the design mode optimization of Nasa Stage 35. Optimization settings are given in Table 2. Solidity and total pressure distributions are represented by Bezier polynomials and the control points of Bezier polynomials are defined as optimization variables. The pareto front obtained from the design mode optimization is given in Figure 12.

Table 2 Design Mode Optimization Variables

Optimization variables (23 variables)	# of variable
rotor solidity distribution	5 control points
stator solidity distribution	5 control points
stage pressure ratio distribution	5 control points
rotational speed	1 value
first stage hub to tip ratio	1 value
inlet axial velocity	1 value
stage axial velocity ratio	1 value
rotor meridional view aspect ratio	1 value
stator meridional view aspect ratio	1 value
meanline radius ratio	1 value
rotor area contraction	1 value

Rotational speed (RPM) is found to be the governing parameter in the optimization. Relation between rotational speed and efficiency is given in Figure 13. Increasing RPM in the arrow direction results in lower efficiency which is related to an increase of inlet relative Mach number. On the other hand high RPM provides the stage to do the pressure rise more easily due to increased tip speed. This is the phenomenon that causes increased stall margin as given in Figure 14 in the arrow direction.

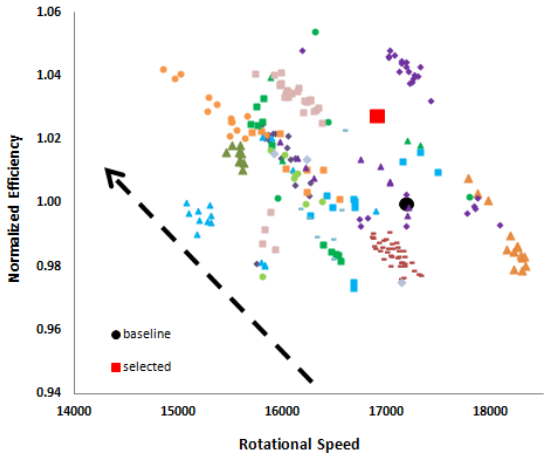

Figure 13 Effect of Rotational Speed on Efficiency

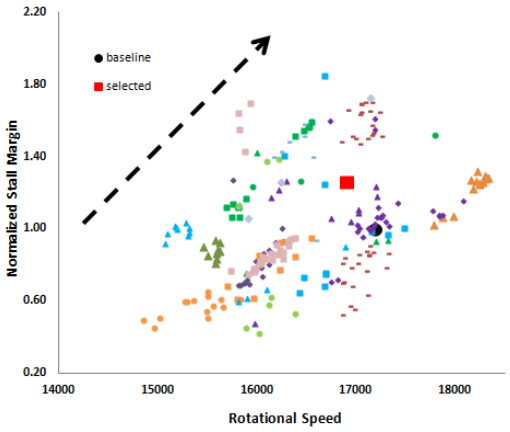

Figure 14 Effect of Rotational Speed on Stall Margin

Optimization Results

This section gives the comparisons between baseline and optimized stages in terms of geometry and performance values. Figure 15 gives the baseline and new rotor geometries. The geometry on the left hand side is the baseline rotor. Second geometry is the rotor from design mode optimization and third geometry on the right hand side is the rotor from analysis mode optimization. Since the third geometry is optimization based with slight changes, the baseline and third geometries are almost identical. Changes can be seen by comparing the tip sections.

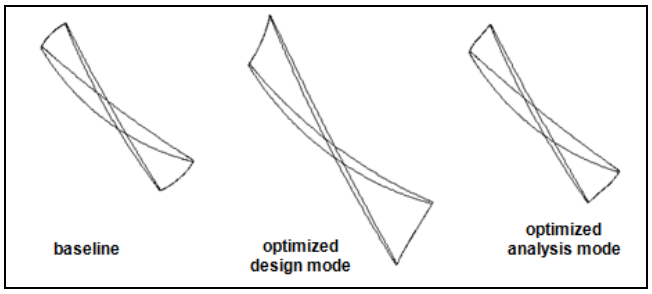

Figure 15 Rotor Blade Comparisons

Figure 16 gives baseline and new flowpaths. Design mode optimized stage has a higher blade hight and lower rotational speed. This flowpath configuration is one of the reasons of reduced losses in design mode optimized geometry since it provides lower inlet relative mach number. Rotor solidity distributions for new geometries are slightly higher at tip as given in Figure 17 which is in favour to reduce losses due to diffusion.

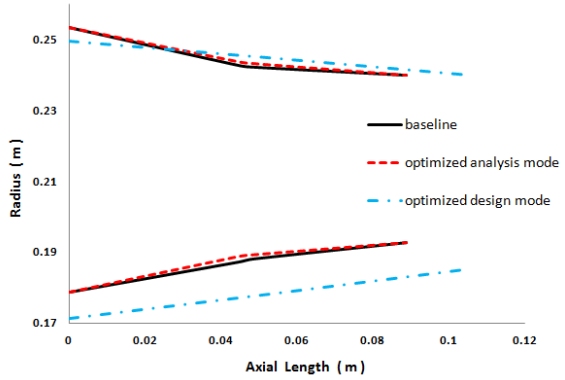

Figure 16 Flowpath Comparisons

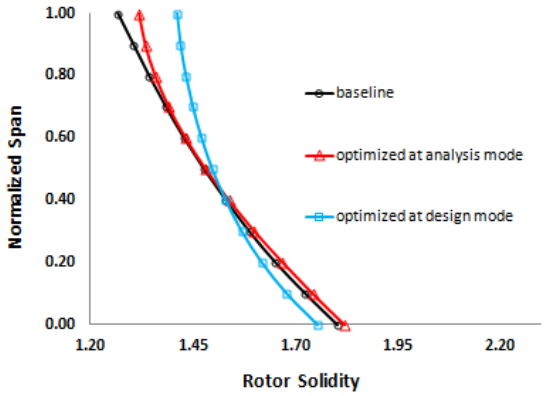

Figure 17 Rotor Solidity Distributions

The CFD performance map comparisons based on stage total to total pressure ratio and stage total to total isentropic efficiency are given at Figure 18 and 19 respectively.

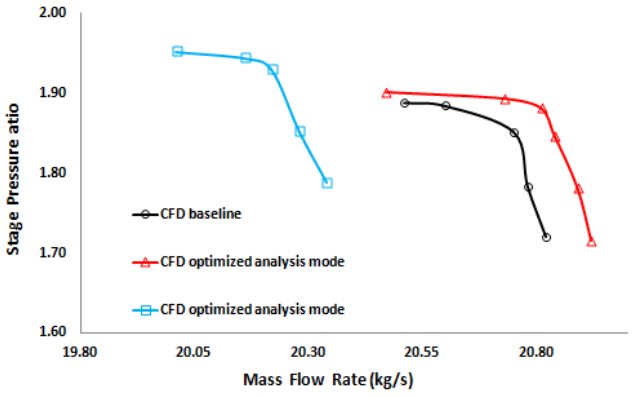

Figure 18 Performance Map, Mass Flow – P.R

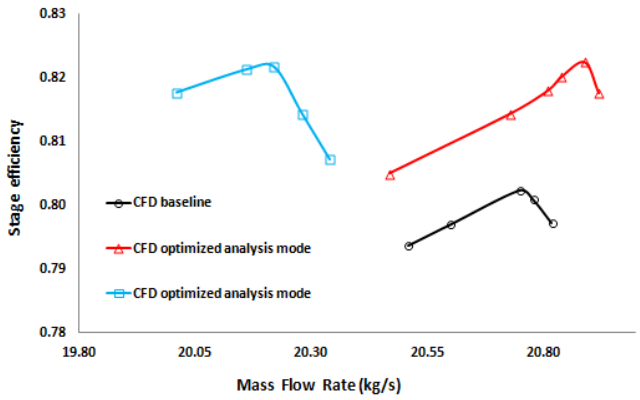

Figure 19 Performance Map, Mass Flow - Efficiency

There are three available stall margin definitions used in the study. The first definition is based only on mass flow rate. This can be considered as constant pressure ratio stall margin. Second definition is based only on pressure ratio which can be considered as constant flow stall margin. Third definition is based on both pressure ratio and mass flow rate. This can be considered as constant rotational speed stall margin. These definitions are given in the following three equations respectively.

$$SM, f(m) = \frac{m_{OP} - m_S}{m_{OP}}.100 \qquad \textbf{Eqn: 2}$$

$$SM, f(PR) = \frac{PR_S - PR_{OP}}{PR_{OP}}.100 \qquad \textbf{Eqn: 3}$$

$$SM, f(m, PR) = \frac{PR_S - 1}{PR_{OP} - 1}.\frac{m_{OP}}{m_S} \qquad \textbf{Eqn: 4}$$

The stall margin based on mass flow rate can be associated with low Mach number operation where the compressor is more tolerant to incidence change which results in a wider performance map in terms of mass flow rate. Stall margin based on pressure ratio can be associated with high Mach number operation where the compressor is less tolerant to change in incidence angle which results in a steeper performance map in terms of mass flow rate. Stall margin based on both mass flow rate and pressure ratio can be considered as a combination of two previous definitions. Since there are different types of stall margin definitions, the final assessment is left to the reader or to the compressor designer. Stall margin improvements in stage performance are given according to CFD calculations in Table 3.

Table 3 Improvements for Stages

	improvement			
geometry	efficiency (%)	SM, f(m) %	SM, f(P.R) %	SM, f(m,P.R) %
baseline	-	-	-	-
design mode optimized	1.51	0.17	3.40	0.08
analysis mode optimized	2.23	0.62	0.98	0.03

The solidity distributions show that the optimized geometries use higher chords. This implies that the expansion on the suction side was tried to be reduced by the throughflow optimization loop. Both optimized stages can reach higher pressure ratios at a higher efficiency with respect to baseline. One should note that baseline performance corresponds to the DCA blading implementation to Stage 35. Since the scope of the study is the meridional optimization, performance comparisons of the optimized geometries with respect to Stage 35 original wedge type bladings will not be given here.

Discussion

When the results are investigated in terms of the main targets of the study, both analysis mode optimization and design mode optimization have provided improvements in stall margin and efficiency. The analysis mode optimization uses the advantage of having a working stage at the beginning and this task aims to improve the existing stage by small modifications. Loss models are exposed to a certain type of geometry so this procedure is ideal for tuning a previously designed compressor geometry at later stages of a design period. The Vital predictions can also be used to support this comment. In the throughflow predictions of Vital, correlations were already user tuned according to the CFD simulation. This validation showed that the throughflow predictions can match with the CFD flow field. On the other hand, the design mode optimization extends the work to a more general solution by setting all the design parameters to free. This creates an aggressive environment for the throughflow code. At design mode optimization, loss models are exposed to different rotational speeds as well as different inlet Mach numbers and different blade heights. So there is a possibility to have different performance between throughflow and 3-D Navier Stokes due to un-tuned loss models. At the performance map comparisons, this can be seen as a reduced mass flow rate in design mode optimized geometry for the same pressure rise. Design mode optimization is ideal for initial phase of a compressor design to provide a reasonable rotational speed and an initial flowpath by a general design space search.

Conclusion

Results of a meridional optimization system for a single stage axial compressor are given where the future target is set to be integrating throughflow and optimization at a multistage level.

A throughflow tool that is developed for the study is based on full radial equilibrium and cascade loss correlations. The tool can operate at both design mode and analysis mode. For validation of the throughflow, two test cases, the high transonic Nasa Stage 35 and EU FP6 Vital low pressure compressor were used. The total loss is represented by the sum of loss sources that are based on diffusion factor, shocks and secondary flows. If the correct group of these models implemented together, successful designs and reliable predictions are possible.

Optimization was done using a genetic algorithm with a weighted sum approach for multi-objective formulation. Performance of the existing single stage compressor was improved with the analysis mode optimization by changing parameters flowpath, blade chord, camber and pitch. A more general task is implemented at design mode optimization by designing a new stage. Full flowpath description, rotational speed, solidity distribution and exit total pressure distribution were the parameters of optimization.

The multi-objective optimization was done to maximize two conflicting parameters namely stall margin and efficiency. For the analysis mode optimization which can be considered as slight improvements for an existing stage, importance of tuning throughflow with CFD analysis is pointed. Design mode optimization can be a good view of design space when the design starts with an empty sheet of paper with less information about flowpath and rotational speed.

References

[1] Chen L., Luo J., Sun F., (2010), Preliminary Design Efficiency Optimization of 1D Multistage Axial Flow Compressor for a Fixed Distribution of Axial Velocities, Revista Termotehnica, No:1

[2] Benini E., (2004), Accurate Multi-objective Design Optimization of Rotor 37, 59th Congresso Annuale ATI, Genova

[3] Keskin A., Bestle D., (2006), Application of Multi Objective Optimization to Axial Compressor Preliminary Design, Aerospace Science and Technology, Vol. 10.

[4] Teichel S., Verstraete T., Seume J., (2013), Optimized Preliminary Design of Compact Axial Compressors, A Comparison of Two Design Tools, 31st AIAA Applied Aerodynamics Conference.

[5] Wu, C., (1952), A general theory of three dimensional flow in subsonic and supersonic turbomachines of axial, radial and mixed flow types, Naca TN 2604. Washington, Naca.

[6] Lieblein S., Schwenk F.C., Broderick R.L., (1953), Diffusion Factor for Estimating Losses and Limiting Blade Loadings in Axial Compressor Blade Elements, NACA RM E53D01.

[7] Hirsch, C., Denton, J.D., (1981), Throughflow calculations in axial turbomachines. London,

[8] Aungier R., (2003), Axial Flow Compressors, A Strategy for Aerodynamic Design and Analysis, ASME Press.

[9] Brouckaert J.F., Van de Wyer N., Farkas B., Capart R., Thomas J.F., Isaac N., Hiernaux S., Perez J.G., (2009), Experimental and Numerical Investigation of a Single Stage Low Pressure Compressor for Counter-Rotating Turbofan Engine Architectures, 8th European Turbomachinery Conference, Graz

[10] Creveling, H., Carmody, R., (1968), NASA CR-54531 Axial Flow Compressor Design Computer Programs Incorporating Full Radial Equilibrium Program 3, Ohio , NASA.

[11] Howel , A., RM-2095, (1942), The Present Basis of Axial Compressor Design Part 1 Cascade Theory. Aeronautical Research Council.

[12] Pachidis P., (2006), Gas Turbine Advanced Performance Simulation, PhD Thesis, Cranfield Unv.

[13] Schwenk F., Lewis G., Hartman M., (1957), Preliminary Analysis of the Magnitude of Shock Losses in Transonic Compressors, NACA RM E57A30.

[14] Reid L., Moore R.D., (1978), Performance of Single Stage Axial Compressor with Rotor and Stator Aspect Ratios of 1.19 and 1.26 and with Design Pressure Ratio of 1.82, NASA TP 1338.

[15] Brouckaert J.F., (2014), Private Communication, von Karman Institute for Fluid Dynamics.

[16] Breugelmans, F., Colpin, J., (1976), Aerodynamic and Mechanical Factors Affecting the Surge Line, VKI CN96

[17] Johnsen I., Bullock R., (1965) , Aerodynamic Design of Axial Flow Compressors, NASA SP-36, Washington